Article

Cell Reports

# Deciphering the Innate Lymphoid Cell Transcriptional Program

## Graphical Abstract

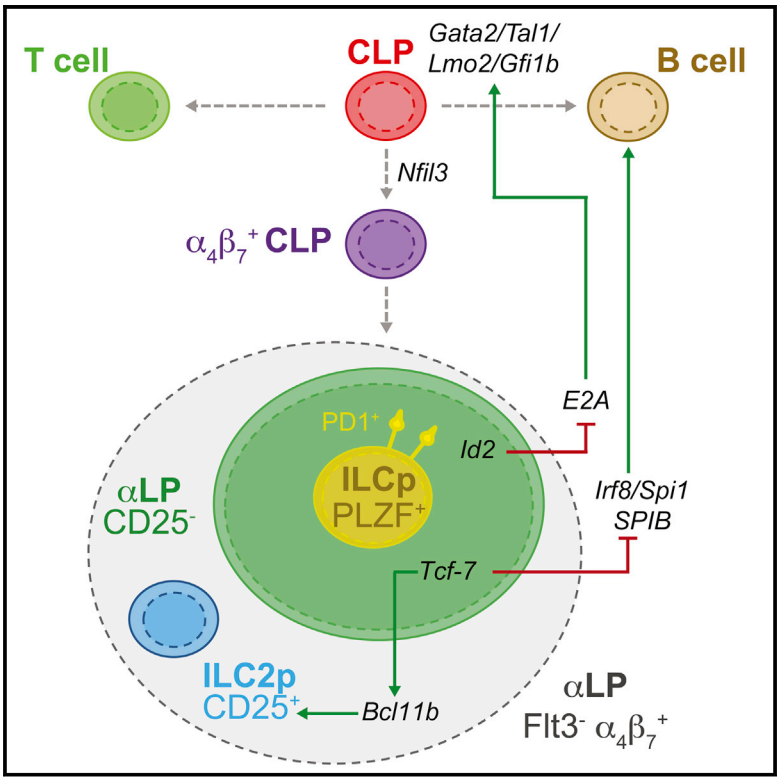


## Highlights

- ILCp transcriptomics define the blueprint for hierarchical ILC development
- PD-1 identifies the PLZF-expressing ILC precursor in the bone marrow
- Transient NFIL3 expression prior to ID2 expression is required for ILC development
- ID2 and TCF-1 are required to extinguish stem cell and B and T cell gene programs

## Authors

Cyril Seillet, Lisa A. Mielke, Daniela B. Amann-Zalcenstein, ..., Nicholas D. Huntington, Sebastian Carotta, Gabrielle T. Belz

## Correspondence

seillet@wehi.edu.au (C.S.), sebastian.carotta@boehringer-ingelheim.com (S.C.), belz@wehi.edu.au (G.T.B.)

## In Brief

Seillet et al. define the hierarchical blueprint for ILC development using global transcriptomic analyses of ILC progenitors. This revealed that PD-1 is a key marker of ILCp and uncovered a regulatory circuit governed by NFIL3 in regulating ID2 and TCF-1 essential for ILC differentiation.

## Accession Numbers

GSE75851

Seillet et al., 2016, Cell Reports *17*, 436–447
October 4, 2016 
http://dx.doi.org/10.1016/j.celrep.2016.09.025

OPEN ACCESS
CellPress

Cell Reports
Article

# Deciphering the Innate Lymphoid Cell Transcriptional Program

Cyril Seillet,[1,2,*] Lisa A. Mielke,[1,2] Daniela B. Amann-Zalcenstein,[1,2] Shian Su,[1,2] Jerry Gao,[1,2] Francisca F. Almeida,[1,2] Wei Shi,[1,2,3] Matthew E. Ritchie,[1,2] Shalin H. Naik,[1,2] Nicholas D. Huntington,[1,2] Sebastian Carotta,[1,4,*] and Gabrielle T. Belz[1,2,5,*]

[1]The Walter and Eliza Hall Institute of Medical Research and Department of Medical Biology, University of Melbourne, Parkville, VIC 3052, Australia
[2]Department of Medical Biology, University of Melbourne, Parkville, VIC 3010, Australia
[3]Department of Computing and Information Systems, University of Melbourne, Parkville, VIC 3010, Australia
[4]Boehringer-Ingelheim RCV, Doktor-Boehringer-Gasse 5–11, 1120 Vienna, Austria
[5]Lead Contact
*Correspondence: seillet@wehi.edu.au (C.S.), sebastian.carotta@boehringer-ingelheim.com (S.C.), belz@wehi.edu.au (G.T.B.)
http://dx.doi.org/10.1016/j.celrep.2016.09.025

## SUMMARY

**Innate lymphoid cells (ILCs) are enriched at mucosal surfaces, where they provide immune surveillance. All ILC subsets develop from a common progenitor that gives rise to pre-committed progenitors for each of the ILC lineages. Currently, the temporal control of gene expression that guides the emergence of these progenitors is poorly understood. We used global transcriptional mapping to analyze gene expression in different ILC progenitors. We identified PD-1 to be specifically expressed in PLZF$^+$ ILCp and revealed that the timing and order of expression of the transcription factors NFIL3, ID2, and TCF-1 was critical. Importantly, induction of ILC lineage commitment required only transient expression of NFIL3 prior to ID2 and TCF-1 expression. These findings highlight the importance of the temporal program that permits commitment of progenitors to the ILC lineage, and they expand our understanding of the core transcriptional program by identifying potential regulators of ILC development.**

## INTRODUCTION

Innate lymphoid cells (ILCs) are enriched at mucosal surfaces and sense inflammatory signals to provide protection from mechanical and pathogenic insults through rapid secretion of cytokines. They develop initially from progenitors in the fetal liver (Chea et al., 2016; Ishizuka et al., 2016) and, later, in the adult bone marrow (BM) (Constantinides et al., 2014; Klose et al., 2014; Yu et al., 2014). Subsequently, ILCs seed mucosal tissues, where they become tissue-resident and continue to proliferate in these tissues to maintain tissue homeostasis. Self-renewal in the localized environment is generally sufficient to deal with acute physiological stressors and infection, but long-term protection requires recruitment of bone marrow-derived progenitors to fully replenish the pool of tissue-resident ILCs.

All ILCs depend on the transcription factors inhibitor of DNA binding 2 (ID2, encoded by *Idb2*) and nuclear factor interleukin 3 (NFIL3) because the deletion of either factor in early lymphoid progenitors severely impairs the development of all ILC subsets. ID2 modulates signaling by heterodimerization with E proteins to prevent initiation of transcription. Constitutive expression of Id2 is subsequently required to maintain ILC3s and ILC1/natural killer (NK) cell homeostasis (Delconte et al., 2016; Guo et al., 2014). In contrast, NFIL3 is essential for the formation of ILC progenitors downstream of the common lymphoid progenitor (CLP) (Seillet et al., 2014a, 2014b) but appears to be dispensable in mature NK cells (Firth et al., 2013). The exact functional relationship between NFIL3 and ID2 is currently incompletely understood. Although it has been proposed that NFIL3 is needed to directly activate ID2 (Male et al., 2014; Xu et al., 2015), ID2 expression is not altered in NFIL3-deficient NK cells (Crotta et al., 2014; Seillet et al., 2014a). TCF-1 (T cell factor 1, encoded by *Tcf7*) has also been shown to be necessary for the ILC differentiation, and its loss affects the differentiation of multiple ILC subsets (Mielke et al., 2013; Yang et al., 2013). The interactions among TCF-1, NFIL3, and ID2 are likely to form a critical decision hub for the differentiation of the earliest bone marrow progenitor cells that give rise to the ILC lineage. Despite this, exactly how the molecular cues of each of these factors are integrated and drive commitment remains unclear.

Here, we utilized a highly purified ILC progenitor called the α-lymphoid precursor (αLP) (Yu et al., 2014) immediately downstream of the CLP to track the transcriptional regulation occurring during ILC commitment. Currently, αLPs are the earliest ILC progenitors described (Yu et al., 2014). This population contains progenitors with a restricted potential and include the common helper innate lymphoid cell progenitor (CHILP) (Klose et al., 2014) and the innate lymphoid cell precursor (ILCp). This progenitor is characterized by expression of the transcription factor PLZF (encoded by *Zbtb16*) and generate ILC1, ILC2, and NKp46$^+$ ILC3 but not NK or lymphoid tissue inducer (LTi)-like cells (Constantinides et al., 2014). Recently, the early ILC

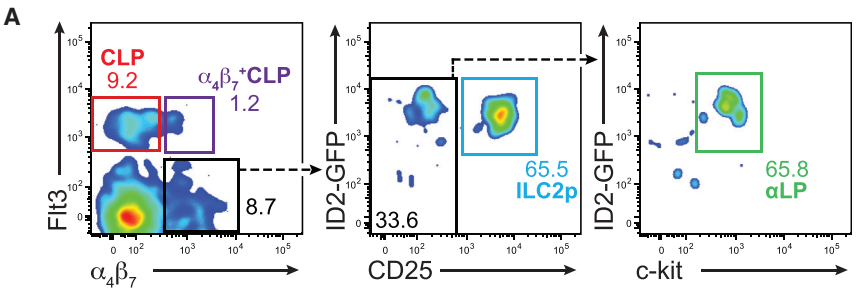


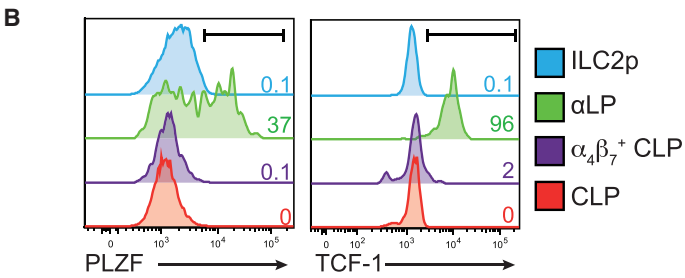


**Figure 1. Identification of Innate Lymphoid Precursors in the Bone Marrow**

(A) Flow cytometric analysis of CLP and αLP bone marrow cells from *ID2*$^{gfp/gfp}$ mice gated on lin$^-$ CD127$^+$c-kit$^{int}$Sca-1$^{int}$ cells. Expression of ID2, CD25, and c-kit is shown within the αLP populations.

(B) Histograms showing the expression of PLZF and TCF-1 in the indicated populations. Data are representative of three similar experiments.

progenitor (EILP), which is characterized by the expression of TCF-1, was found to be able to give rise to NK cells and all known ILC lineages (Yang et al., 2015). However, the EILP is distinct from all other ILC precursors because it does not express CD127. Whether EILP represent an alternate pathway for ILC differentiation remains to be determined (Zook and Kee, 2016) because it does not fit the current linear model of ILC differentiation in which all ILC precursors express CD127 (IL-7R), which is essential for development into mature cells in the periphery. We therefore chose to focus our analyses on IL-7Rα-expressing progenitors.

Using whole-genome analyses of in-vivo-derived cells, we demonstrate that *Tcf7* and *Nfil3* are essential for the transition of CLP to the αLP and the induction of an ILC-specific transcriptional program. We identified several transcription factors that have not been associated previously with ILC development. These included *Maf*, *Zbtb7b*, and *Ikzf2*. Strikingly, *Nfil3* was required only transiently at the earliest stages of ILC development, whereas *Id2* drove ILC differentiation, at least in part, through the repression of genes associated with stem cell maintenance and B and T cell differentiation. Collectively, we define the transcriptional landscape of ILC precursors and provide insight into the interplay of transcription factors, particularly the hierarchical interactions, among *Id2*, *Nfil3*, and *Tcf7* utilized by progenitor cells to generate ILC populations.

## RESULTS

### Verification of Progenitors for Transcriptional Analyses

Initially, we confirmed the differentiation potential of several progenitor stages for ILCs to ensure that our transcriptional analyses would map accurately to the starting populations and the mature differentiated cells they produced. The αLP (defined as lin$^-$Flt3$^-$c-kit$^{int}$Sca-1$^{int}$CD127$^+$α$_4$β$_7^+$ cells) is the earliest lymphoid progenitor that lacks B and T cell potential (Possot et al., 2011; Yu et al., 2014). Analyses of the αLP in bone marrow of ID2$^{gfp}$ reporter mice using a gating strategy similar to that reported previously showed that this population included some CD25$^+$ ILC2 progenitors (ILC2p) (Figure 1A; Hoyler et al., 2012). The remaining αLP (CD25$^-$) showed heterogeneous expression of PLZF but uniformly expressed TCF-1 (Figure 1B) similar to the recently described early ILC progenitors known as the EILP (Yang et al., 2015). Therefore, the αLP contains both the CHILP (Klose et al., 2014) and PLZF$^+$ ILCp (Constantinides et al., 2014), as reported previously (Yu et al., 2014).

To confirm the lineage potential of the different progenitors that we proposed to analyze using global gene profiling, we transferred ~1,000 purified, congenically marked (CD45.1$^+$) CLP (Kondo et al., 1997), α$_4$β$_7^+$ CLP (Ishizuka et al., 2016) (a small population of cells that coexpressed both FLT3 and α$_4$β$_7$), αLPs (that lacked CD25$^+$ cells), or ILC2ps (Hoyler et al., 2012; Table S1; Figure S1) into sublethally irradiated *Rag2*$^{-/-}$ γ$_c^{-/-}$ mice (CD45.2$^+$). As expected, CLP gave rise to all lymphoid populations (Figure S2A), whereas ILC2p only generated the ILC2 lineage (data not shown). Interestingly, the α$_4$β$_7^+$ CLP generated all ILC subsets but retained the capacity to form a small fraction of T and B cells, similar to their recently reported in vitro potential (Figure S3; Ishizuka et al., 2016). This effect could be attributable to the lack of expression of Id2 at this stage of development.

The αLP did not generate B cells or T cells but was able to differentiate into all ILC subsets in the small intestine (Figure S2A). In the liver, the αLP efficiently gave rise to both TRAIL$^-$CD49b$^+$ NK cells and TRAIL$^+$CD49b$^-$ ILC1 (Figure S2B), a feature confirmed using our dual reporter ID2$^{gfp}$ × eomesodermin (EOMES)$^{mCherry}$ mice to directly track these cells (Figures S2C and S2D). Interestingly, in the spleen, only ID2$^+$EOMES$^+$ NK cells were generated from αLP, indicating that the microenvironment likely plays an important role in supporting the development of ILC1 (Figure S2D).

### Transcriptional Dynamics of Innate Lymphoid Cell Development

The precise molecular events that occur during ILC lineage commitment are poorly understood. Using the αLP as defined above without ILC2p contamination (Table S1; Figure S1), we

sought to map the earliest transcriptional changes during ILC commitment. Transcriptional analyses of small numbers of the CLP and each ILC developmental stage (namely, the $\alpha_4\beta_7^+$ CLP, the αLP, and ILC2p [CD25$^+$]; Table S1) was performed to map gene expression changes during ILC development. Because each of these precursors represent extremely infrequent populations, we performed RNA sequencing (RNA-seq) analysis on 100 cells using the recently described cell expression by linear amplification and sequencing (CEL-seq) protocol (Hashimshony et al., 2012).

Non-supervised hierarchical clustering and multi-dimensional scaling (MDS) revealed that biological replicates clustered tightly and did not overlap between the different purified populations, confirming the quality of CEL-seq analysis, the purity of the sorts, and that the gating strategy captured distinct populations (Figure 2A). We found that the $\alpha_4\beta_7^+$ CLP clustered closely with the CLP, implying a close developmental relationship between these populations. We therefore focused our analysis on the transcriptional changes that occurred during the transition between CLP, αLP, and ILC2p. Overall, 462 genes were differentially regulated between the CLP and αLP stage (Figure 2B). Among those, 251 transcripts were upregulated during the transition from CLP to αLP, and 211 genes were downregulated. Genes differentially regulated included the previously published key ILC commitment factors *Id2*, *Gata-3*, *Tox*, and *Tcf7*. Importantly, we also found genes such as Arginase-1 (encoded by *Arg1*), *Lmo4*, *Socs1*, and *Tox2*, which were all upregulated during the transition from the CLP to αLP stage.

In the transition from the αLP toward the ILC2p, 97 genes were upregulated, whereas 363 genes were downregulated, indicating that a key requirement for the development of ILC2 subset was the repression of alternative lineage potential, such as Sox4 (Schilham et al., 1996) or Myb (Allen et al., 1999), because both genes have been implicated previously in B cell and T cell development. In the transcripts showing expression more than 4-fold higher than in the αLP, we found several markers characteristic of ILC2, including *Il1rl1*, *Il2rα*, *Ly6a*, *CCR9*, and *Klrg1* as well as transcripts such as *Socs2*, *Cysltr1*, *Cish*, *Traf4*, and *Rnf128* (Figure 2C).

To monitor global transcriptional changes, we generated a heatmap of gene sets for precursor-product transitions that identified genes with significantly different expression in two developmentally related populations (false discovery rate [FDR] < 0.05) (Figure 2D). This allowed us to better visualize the magnitude and number of transcripts induced or repressed at each transition. The heatmap clearly revealed unique gene signatures characteristic of each specific developmental stage. To precisely identify the dominant transcriptional programs present in the early innate lymphoid progenitors, we applied a K-means clustering algorithm to the set of differentially regulated genes that allows unsupervised pattern recognition (Figures 2E and S4; Table S2). Thus, these analyses provide a rich resource for discovering additional molecular actors in ILC development. The first two clusters showed a down-modulation of genes. Cluster 1 was associated with genes involved in early development and differentiation, including the transcription factor *Sox4*, the retinoid-inducible nuclear factor *Cxxc5*, and the core binding factor *Cbfa2t3*, which is able to interact with DNA-bound transcription factors to facilitate transcriptional repression. Genes in cluster 2 showed a strong downregulation from the CLP stage to ILC progenitors and were associated with reduced expression of T- and B cell-associated genes such as *Blnk*, *Spib*, *Rag1*, and *Lmo2.* In contrast, cluster 3 included genes that were upregulated after the CLP stage in αLP and generally maintained or increased their expression in ILC2p. This cluster included several genes encoding key transcriptional regulators of ILC development, including *Id2* and *Gata-3*, which have broad effects on multiple ILC subsets. Cluster 4 grouped genes that are upregulated in ILC2p, such as *Il1rl1* and *Il2rα*, together with genes of unknown function in ILC2 biology, including *Cish*, *Socs2*, or *Tgfbr1*. Cluster 5 included genes that are temporally upregulated in αLP and contained genes such as *Rorc*, *Rora*, *Tcf7*, *Tox*, and *Eomes*, all transcription factors that are associated with specific ILC subsets. The expression of genes that are important for ILC subset specification suggests that priming into the different ILC lineages already occurs at the αLP stage and may explain why fewer than 10% of the ILC progenitors give rise to all ILC subsets at a clonal level (Possot et al., 2011; Yu et al., 2014). Support for this hypothesis comes from a recent single-cell analysis of fetal liver-derived ILC precursors that demonstrated mixed ILC1, ILC2, and ILC3 transcriptional patterns (Ishizuka et al., 2016). Cluster 6 is similar to cluster 5 in that genes were strongly downregulated during ILC2p commitment but did not show such strong upregulation at the αLP stage, similar to cluster 5. This cluster consisted of a number of surface molecules such *as Il18r1*, *Nkg7*, *Klrb1f*, and *Klrd1* or altered intracellular trafficking and metabolism such as *Galk2* and *Unc119b*. Collectively, these patterns identify discrete steps in commitment to mature ILC lineages.

## Identification of Early Regulators of Commitment in Innate Lymphoid Precursors

To characterize the molecular profile of the αLP in more depth, we focused our analysis on genes that were upregulated from the transition of CLP to αLP and divided genes according to their biological function defined in the Molecular Signatures Database (MSigDB) (Figure 3A). First, we examined transcription factors based on their role as key regulators of lineage commitment. As expected, we found that genes encoding molecules with previously assigned functions in ILC differentiation, such as *Id2*, *Tox*, *PLZF*, *Gata-3*, and *Tcf-7*, were strongly modulated (Figure 3A). This expression was reflected in upregulation of protein expression for TCF-1, PLZF (Figure 1A), LMO4, and GATA-3 (Figure 3B) and the sequential downregulation of factors such as PU.1 and IRF8 as ILC progenitors undergo commitment (Figure 3B). Although PU.1 expression was downregulated in αLP compared with CLP, all αLPs still expressed an intermediate level of PU.1, a feature that could be used as an interesting molecular marker to identify this precursor. Genes such as *Rxrg*, *Zbtb7b*, *Maf*, *Ikzf2*, and *Tox2* will require more extensive investigation to identify their role in ILC differentiation (Figures 2D and 3A).

Among surface markers, we identified several immunoregulatory molecules, including the tumor necrosis factor (TNF) superfamily genes *Tnfsf14* (encoding Light) *Tnfsf25* (encoding Leaf), CD160, *Nt5e* (CD73), ICOS, and CD226 (DNAM-1) and the

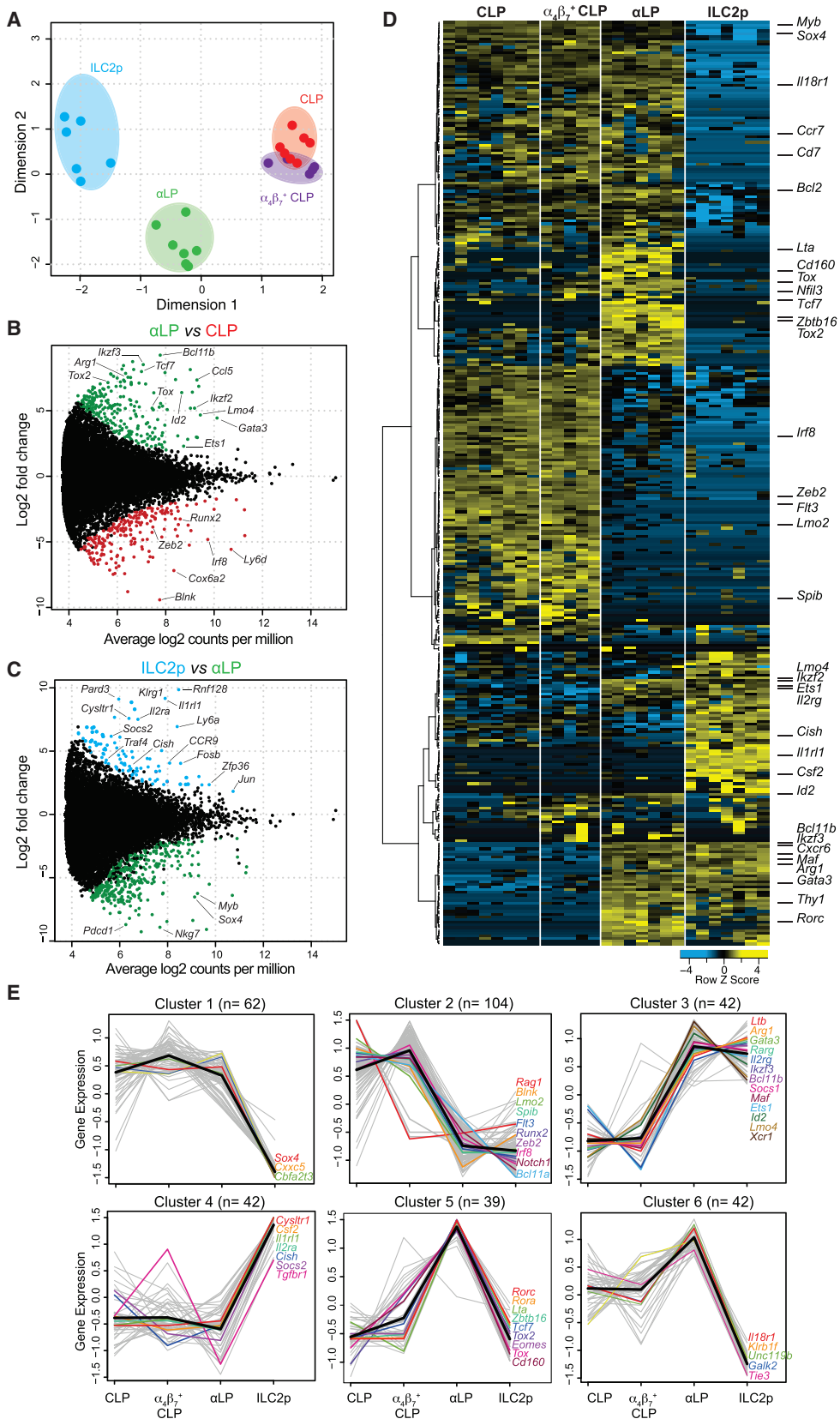


*(legend on next page)*

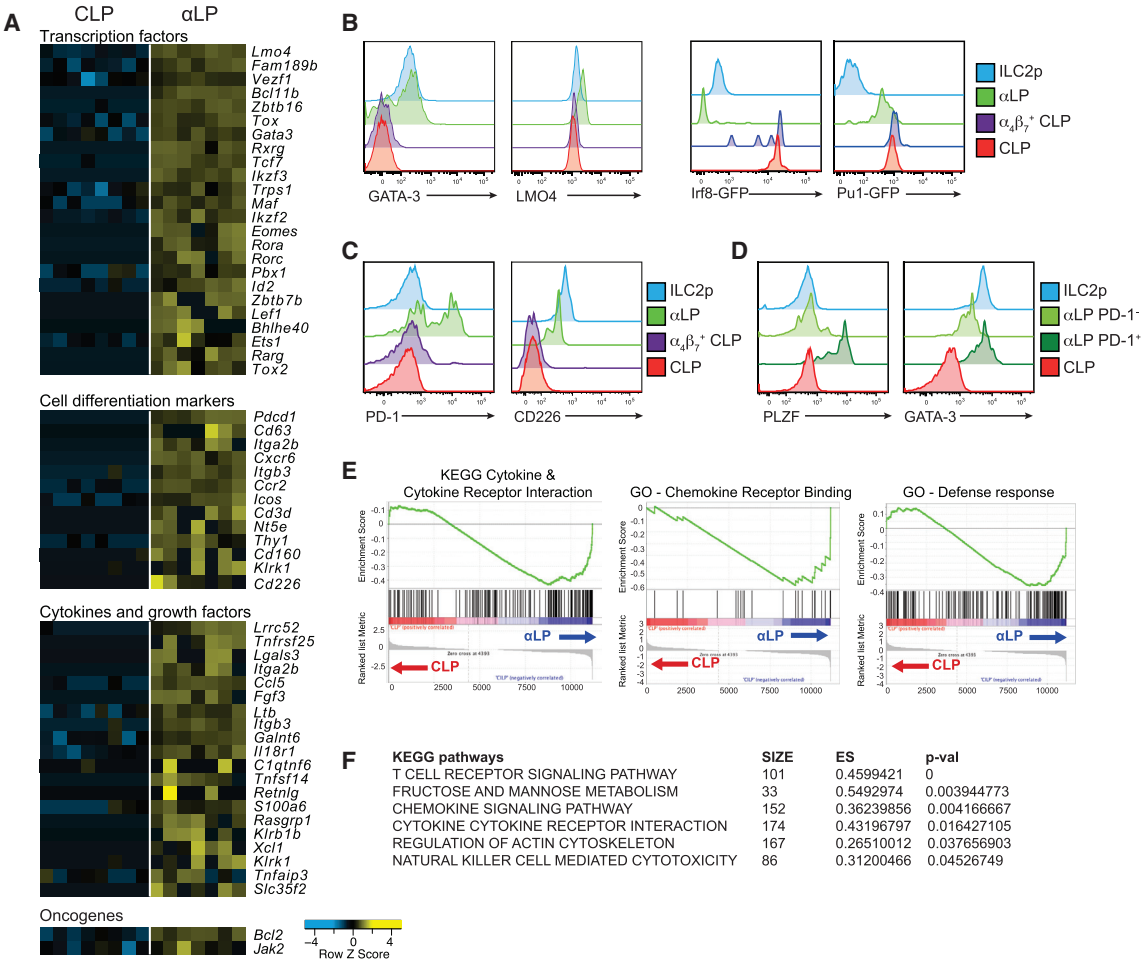


**Figure 3. Molecular Characterization of the αLP**

(A) Heatmap representation of genes with at least 2-fold differences in expression pattern between CLP and αLP. Columns represent the indicated cell subsets in seven to eight biological replicates. Gene sets are clustered according to their biological function based on the gene families of the MSigDB database.

(B and C) Histograms show intracellular expression of (B) GATA-3 and LMO4 (left) and GFP expression of IRF8$^{gfp/+}$ and PU.1$^{gfp/+}$ reporter mice (right) and (C) surface expression of PD-1 and CD226 in the indicated populations. Data are representative of two independent experiments (n = 2–3 mice/experiment).

(D) Histograms showing intracellular expression of PLZF and GATA-3 in the PD1$^{+}$ and PD1$^{-}$ fraction of the αLP. Data are representative of two independent experiments (n = 2 mice/experiment).

(E) GSEA was performed to compare the CLP and αLP transcriptional profile with the KEGG and the MSigDB C5 GO.

(F) KEGG pathways are significantly enriched in αLP.

inhibitory receptor PD-1 (programmed cell death protein 1) (Figures 3A and 3C). Flow cytometric analysis showed that CD226 was expressed uniformly on the αLP and that this was maintained on ILC2p, whereas the expression of PD-1 on αLP was heterogeneous and downregulated on ILC2p (Figure 3C). Because PD-1 was expressed only in a fraction of the αLP, we wondered whether this marker could be used to discriminate precursor subsets known to be contained in the αLP, such as

**Figure 2. The Transcriptional Landscape of ILC Development**

CEL-seq analysis was performed on highly purified precursors as defined in Figures 1 and S2.

(A) MDS of the CEL-seq results obtained from the CLP (red), α4β7$^{+}$ CLP (purple), αLP (green), and ILC2p (blue) populations. Each point represents a different sample, and samples are color-coded by population.

(B and C) Comparison of gene expression in (B) αLP versus CLP cells and in (C) ILC2p versus αLP in smear plots. Colored dots indicate genes significantly upregulated in CLP (red), αLP (green), and ILC2p (blue).

(D) Heatmap showing the differentially expressed genes across ILC progenitor developmental stages. Data were row-normalized and hierarchically clustered by gene and subset. Genes are color-coded (see legend) to display relative gene expression.

(E) K-means clustering into six clusters based on expression pattern during early ILC differentiation. Shown is the expression of genes (log2-transformed mean-centered, gray lines) and cluster centroids (black line) for each cluster.

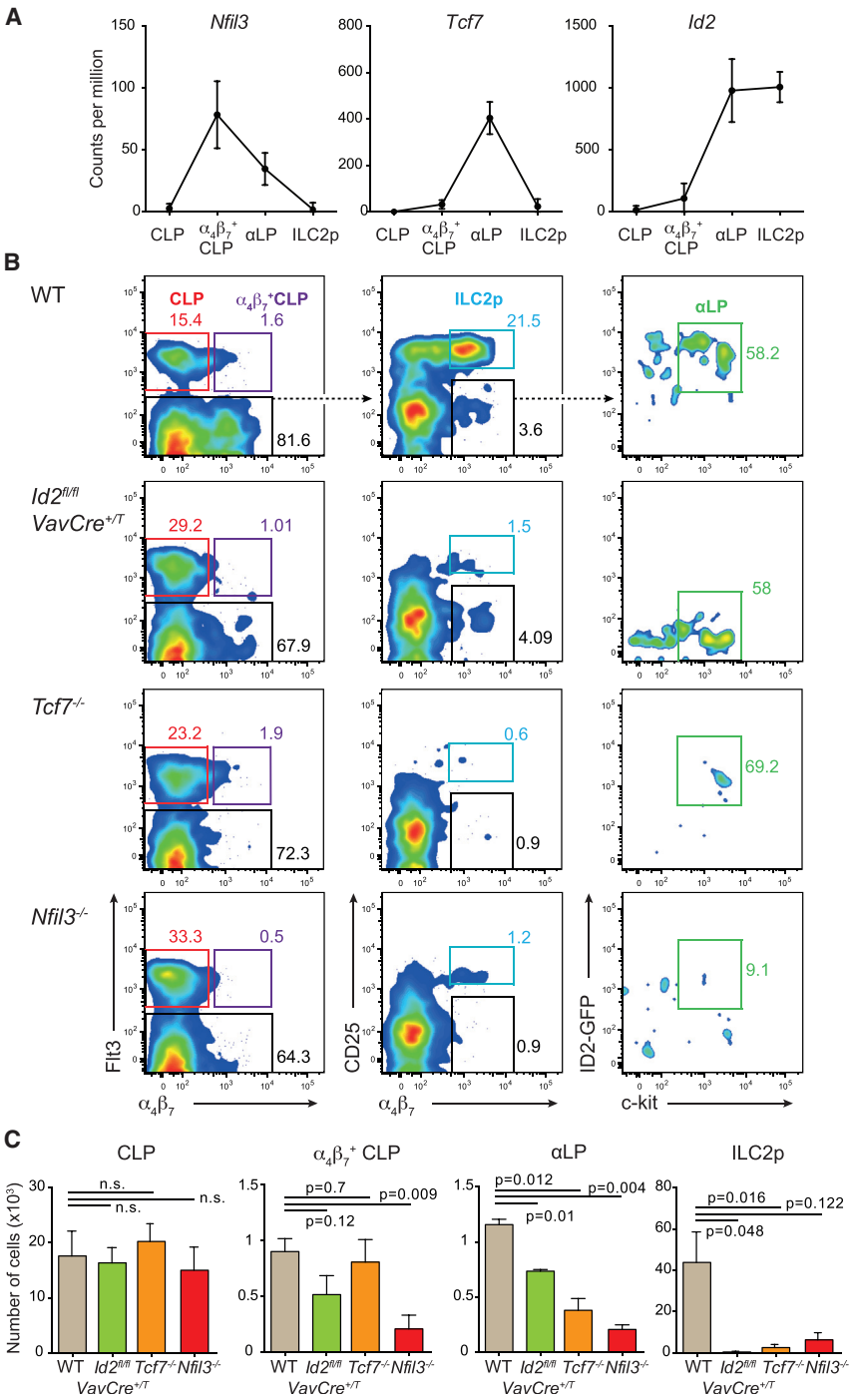


**Figure 4. Development of ILC Precursors Gradually Depends on *Nfil3*, *Tcf7*, and *Id2***

(A) Counts per million mapped reads for *Nfil3*, *Tcf7*, and *Id2* in CLP, $\alpha_4\beta_7^+$ CLP, αLP, and ILC2p are shown (mean ± SD).

(B) Flow cytometric analyses of lineage$^-$ bone marrow cells from wild-type (WT), *Id2*$^{fl/fl}$*VavCre*$^{+/T}$, *Tcf7*$^{-/-}$, and *Nfil3*$^{-/-}$ mice. The profiles show the frequency of each progenitor subset gated on live lin$^-$ CD127$^+$ cells. The data show one of two representative experiments.

(C) Total cell number of the indicated populations isolated from wild-type, *Id2*$^{fl/fl}$*VavCre*$^{+/T}$, *Tcf7*$^{-/-}$, and *Nfil3*$^{-/-}$ mice. The data show the mean ± SD pooled from two independent experiments (n = 4).

the PLZF$^+$ ILCp (Constantinides et al., 2014; Yu et al., 2014). Interestingly, the PD1$^+$ fraction of the αLP contained PLZF- and Gata3-expressing cells, indicating that PD-1 specifically identify the ILCp (Figure 3D). Despite this distinct expression pattern of PD-1, however, analysis of *Pdcd1*$^{-/-}$ mice demonstrated that PD-1 expression is not essential for the formation of the αLP and does not affect the development of mature ILC at steady state (Figure S5). Thus, PD-1 and CD226 represent important markers for the identification of αLP that will allow the isolation of these cells without the use of reporter mice for ID2 or PLZF.

To gain further insight into the biological processes controlled by differential gene expression between the CLP and αLP, gene set enrichment analysis (GSEA) was performed (Figures 3E and 3F). We used all pathways in the Kyoto Encyclopedia of Genes and Genomes (KEGG) as well as gene ontology (GO) from the MSigDB C5 database. Both analyses revealed a significant enrichment for cytokine and chemokine-mediated signaling pathways and molecules involved in immune protection and defense (Figures 3E and 3F). These analyses indicate that the αLP differs significantly from the CLP and has already started to acquire a profile consistent with differentiation toward effector lineages.

## Understanding Transcriptional Initiation in ILC Progenitors

Although ID2, NFIL3, and TCF-1 have all been identified as key regulators of early ILC and NK cell differentiation, the kinetic of expression and how these transcription factors are regulated during ILC commitment is unknown. Our analysis revealed that the expression of these factors is tightly regulated during ILC development (Figure 4A). None of these factors were expressed in CLP; however, *Nfil3* was already induced in the $\alpha_4\beta_7$-expressing CLP fraction and was subsequently downregulated in latter progenitors, supporting the notion that early induction of *Nfil3* is necessary for ILC development (Seillet et al., 2014b). *Tcf7* and *Id2* were both strongly induced in the αLP, whereas ID2 expression was maintained in ILC2p, but *Tcf7* expression was downregulated (Figure 4A). These data suggest that each of these factors play an important role at distinct checkpoints

in ILC development. We therefore performed a detailed analysis of the early progenitor stages in the bone marrow of NFIL3-, ID2-, and TCF-1-deficient mice (Figure 4B).

Consistent with lack of mRNA expression of *Nfil3*, *Id2*, and *Tcf7* at the CLP stage, the formation of CLP was not affected when these transcription factors were deleted (Figure 4B). This was not the case for the $\alpha_4\beta_7^+$ CLPs, which were significantly reduced in *Nfil3*$^{-/-}$ mice, mirroring the increased *Nfil3* observed in our analyses (Figures 4A and 4B). We observed a gradual loss of ILC progenitors in the different knockout mice with defects in *Nfil3*$^{-/-}$ > *Tcf7*$^{-/-}$ > *Id2*$^{-/-}$, suggesting different temporal requirements for these transcription factors as they transition between each developmental stages (Figure 4C). Similar defects were also observed in mature cells in chimeric mice reconstituted with transcription factor-deficient bone marrow (Figure S6) indicating that the observed effects were cell-intrinsic. Unexpectedly, the αLP was less affected in *Id2*$^{fl/fl}$*VavCre*$^{+/T}$ mice compared with *Tcf7*$^{-/-}$ and *Nfil3*$^{-/-}$ mice, indicating that ID2 is not required for the formation of the αLP but acts downstream of this stage (Figure 4C).

Because *Nfil3* was only transiently expressed in ILC progenitors, we questioned whether NFIL3 was required for the subsequent maintenance of the ILC differentiation program. We generated *Nfil3*$^{fl/fl}$*Id2-CreERT2*$^{+/T}$ mice to allow spatiotemporal deletion of NFIL3 in ID2-expressing cells. αLPs were purified from *Nfil3*$^{fl/fl}$*Id2-CreERT2*$^{+/T}$ mice and subsequently cultured on OP9 stromal cells in the presence of interleukin-15 (IL-15) or IL-33 and 4-hydroxytamoxifen (4-OHT) or ethanol (control) to drive the differentiation of either ILC1/NK cells or ILC2. Surprisingly, deletion of NFIL3 in ID2$^+$ cells had no apparent effect on the development of the ILC under either ILC1 or ILC2 conditions (Figures 5A and 5B). Both the frequency and the number of ILC1 or ILC2 generated in vitro were similar in both the 4-OH-treated and control cultures (Figures 5A–5C). Deletion of *Nfil3* in these cells, however, was complete (Figure 5D). We next assessed whether mature ILC populations would be maintained in vivo in the absence of *Nfil3* following induction of ID2. Strikingly, the loss of *Nfil3* in these mice did not alter the number of mature ILC1, 2, and 3 in the mesenteric lymph nodes (Figure 5E) or small intestine (data not shown) or the expression of Gata-3 or Rorγt, which are important to maintain the identity of ILC2 and ILC3, respectively. Furthermore, NK cells and ILC1 were unaffected in the liver (Figure 5E) and the spleen (data not shown), indicating that ablation of NFIL3 after ID2 induction does not affect their formation or maintenance. Because the onset of ID2 expression occurs very early in ILC development, this implies that NFIL3 only acts during the transition from the CLP to the αLP. Similar to our findings in in vitro cultures, in vivo treatment with tamoxifen efficiently induced deletion of *Nfil3* specifically in ID2-expressing cells, whereas we could not detect any deletion in ID2-negative cells such as naive T cells (Figure 5F). Thus, NFIL3 is a key factor for the formation of the $\alpha_4\beta_7^+$ CLP and the αLP but is dispensable after the onset of ID2 expression.

Because the induction of *Nfil3*, *Id2*, and *Tcf7* represents the first molecular steps for ILC development, we endeavored to comprehensively profile the genes regulated by these transcription factors in αLP at a genome-wide level. Although the CEL-seq protocol allows transcriptomic analysis on a very small amount of RNA, the defect in NFIL3-deficient mice was so profound that it precluded the generation of libraries of sufficient quality for further analyses. Therefore, we focused our analysis on the remaining αLP found in the ID2- and TCF-1-deficient mice (Figures 6A and 6B). Using this approach, we identified 127 differentially regulated genes in *Id2*$^{-/-}$ αLP and 110 genes in *Tcf7*$^{-/-}$ αLP compared with their wild-type counterparts. Interestingly, few shared genes were found to be differentially regulated between ID2- and TCF-1-deficient cells, suggesting that these two transcription factors control distinct transcriptional programs during ILC development (Figures 6C and 6D). The requirement for these two transcription factors for the full expression of the signature genes of the αLP was highlighted by the significant downmodulation of the expression of the majority of genes found in the αLP signature (Figures 6E and 6F). Several genes identified in this signature were downregulated in the absence of ID2, including *Tox*, *Gata-3*, *Arg1*, and *Lmo4*, suggesting that these factors are within an ID2-regulated pathway and that ID2 is required for their continuous expression. Loss of ID2 also correlated with an increase in many genes normally repressed after transition from the CLP (Figure 2). These included *Gfi1b*, *Tal1*, *Lmo2*, *Gata-2*, and *Hhex*, which are known to have important functions in hematopoietic progenitors (Figure 6A; Table S3). Gene set enrichment analysis using published cluster genes associated with stem cell or pro-B cell signatures (Mingueneau et al., 2013; Revilla-I-Domingo et al., 2012) revealed that genes repressed by ID2—i.e., those upregulated in ID2-deficient αLP in comparison with wild-type αLP—were enriched for hematopoietic progenitor cell or signature genes (Figure 6E). Notably, *Tal1*, *Gfi1b*, and *Bcl11a* are already known to be targets of E protein regulation (Lécuyer et al., 2007; Lin et al., 2010; Xu and Kee, 2007). Thus, ID2 induction is accompanied by a major regulatory shift with broad repression of progenitor cell transcription factor genes to foster ILC lineage commitment and induce critical regulators such as *Tox* and *Gata-3* (Figure 6A). Similar to the loss of ID2, in the absence of *Tcf7*, *Hhex* and *Lmo2*, two genes known to be involved in stem cell function, were upregulated in addition to genes linked to the B cell program, such as *Spib*, *Irf8*, or *Ly6d*. Gene set analysis confirmed the enrichment of unregulated genes associated with a pro-B cell signature (Figure 6F). In contrast, *Bcl11b* was downregulated only in *Tcf7*$^{-/-}$ αLP, consistent with a loss of ILC2 in *Tcf7*$^{-/-}$ mice (Mielke et al., 2013). This suggests that *Tcf7* expression actively represses gene expression programs to allow differentiation of ILC.

## DISCUSSION

The recent identification of committed ILC progenitors in the bone marrow has opened new opportunities to understand how the innate lymphoid lineage emerges during hematopoiesis. However, the rarity of these precursors in vivo has complicated the analysis of the transcriptome of these cells. We used CEL-seq technology to perform full RNA sequencing on different ILC populations and identify transcriptional transitions associated with the lineage progression of innate lymphocytes.

To identify the very first transcriptional changes occurring during ILC specification, we performed a comprehensive transcriptional analysis of various progenitor stages using RNA-seq,

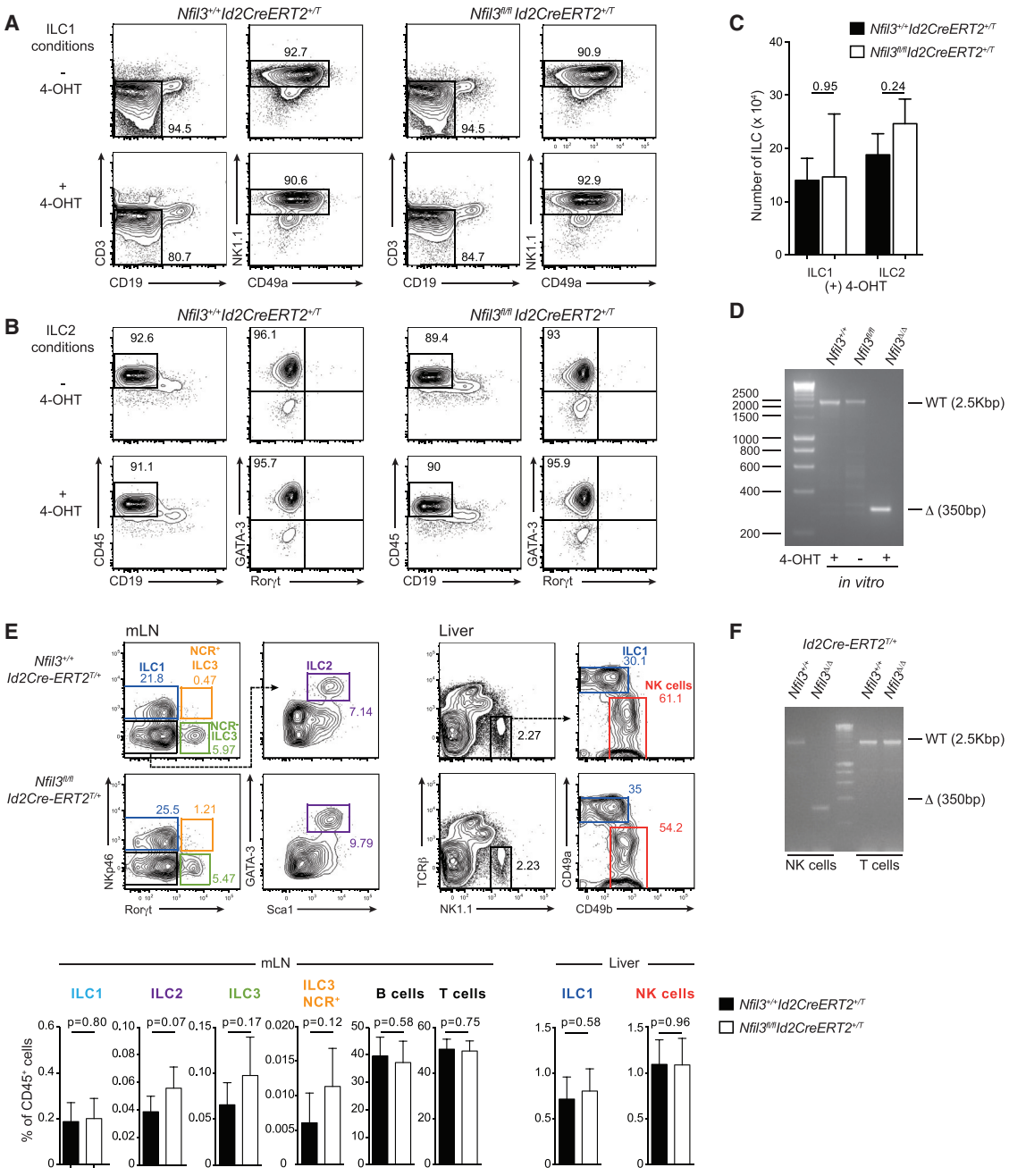


**Figure 5. Transient Expression of Nfil3 Is Sufficient to Induce Commitment to the ILC Lineage**

(A and B) Purified αLP from *Nfil3*$^{+/+}$*Id2CreERT2*$^{+/T}$ and *Nfil3*$^{fl/fl}$Id2CreERT2$^{+/T}$ mice were cultured with IL-7, stem cell factor (SCF(, and either (A) IL-15 or (B) IL-33 to promote their differentiation into ILC1/NK cells or ILC2, respectively. Cells were cultured for 10 days in the presence or absence of 4-OHT as indicated. Expression of NK1.1, CD49a, RORγt, and GATA-3 was analyzed by flow cytometry to track differentiation of NK cells, ILC1, ILC2, and ILC3. The profiles show one representative of two experiments with similar findings.

(C) Total number of ILC1 and ILC2 recovered after 4-OH treatment of *Nfil3*$^{+/+}$*Id2CreERT2*$^{+/T}$ and *Nfil3*$^{fl/fl}$*Id2CreERT2*$^{+/T}$ cells in vitro. The data show the mean ± SD pooled from two independent experiments (n = 4).

(D) Deletion of the *Nfil3* allele was analyzed using PCR on purified NK cells cultured from *Nfil3*$^{fl/fl}$*Id2CreERT2*$^{+/T}$ or *Nfil3*$^{+/+}$*Id2CreERT2*$^{+/T}$ cells with or without treatment with 4-OHT. Ladder, 10 kb.

(E and F) *Nfil3*$^{fl/fl}$*Id2CreERT2*$^{+/T}$ and control *Nfil3*$^{+/+}$*Id2CreERT2*$^{+/T}$ mice were treated with tamoxifen for 10 days, and ILC1, 2, and 3 were analyzed in the mesenteric lymph nodes (mLN) (left) and liver (right).

(E) Histograms show the mean frequency of cells ± SD of data pooled from two independent experiments (n = 6 mice/genotype). Profiles are gated on CD45$^{+}$CD19$^{-}$CD3$^{-}$ cells.

(F) Deletion of the *Nfil3* allele was analyzed using PCR on purified NK cells or T cells from mice analyzed in (E). Ladder, 10 kb.

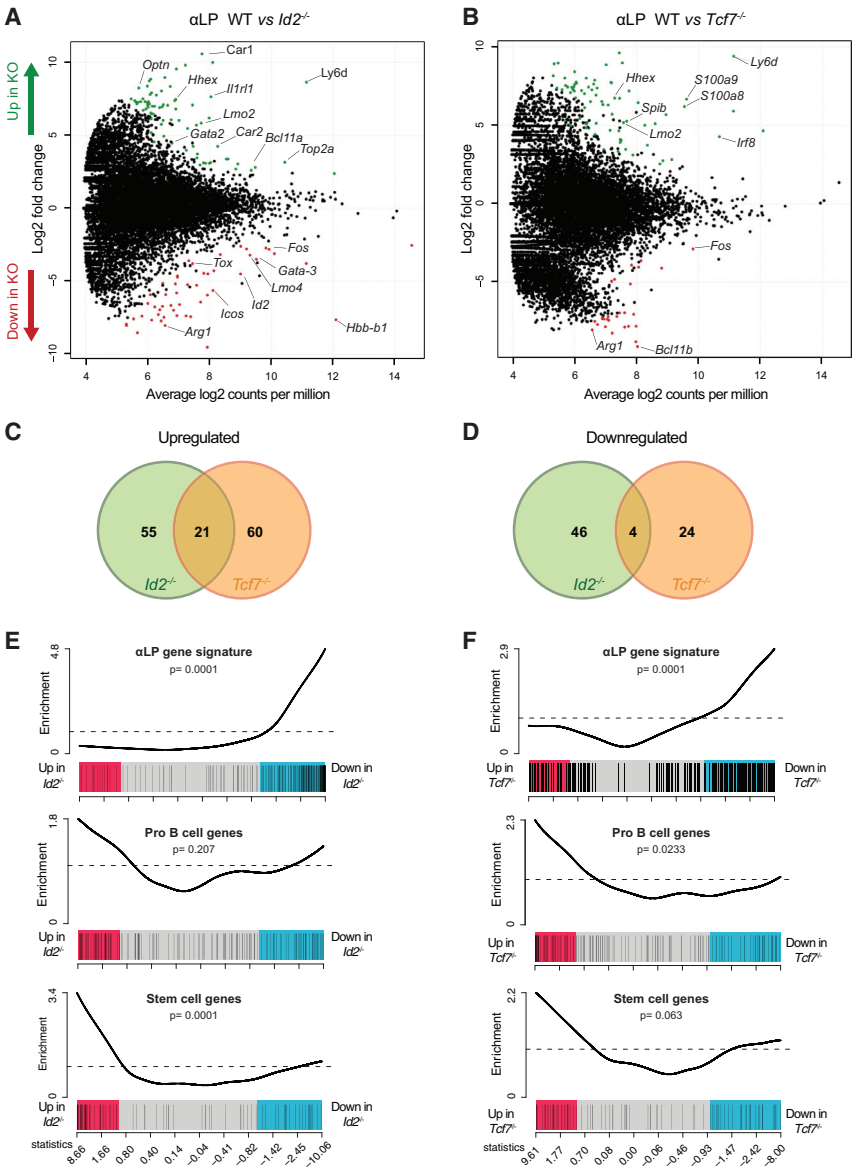


**Figure 6. Id2 and *Tcf7* Regulate Distinct Transcriptional Programs to Repress Stem Cell, B Cell, and T Cell Potential**

(A and B) Comparison of gene expression between αLP from (A) WT and $Id2^{fl/fl}VavCre^{+/T}$ ($Id2^{-/-}$) cells and in (B) WT and $Tcf7^{-/-}$ mice shown in smear plots.

(C and D) Venn diagrams showing unique and overlapping genes. Shown are (C) upregulated and (D) downregulated genes in $Id2^{-/-}$ and $Tcf7^{-/-}$ αLP. Complete lists of genes in each Venn category are listed in Table S3.

(E and F) Gene set enrichment analysis of genes (shaded rectangles,horizontally ranked by moderated *t* statistic) upregulated (pink, $t > 1$), downregulated (blue, $t < -1$), or not altered (gray) in $Id2^{-/-}$ and $Tcf7^{-/-}$ αLP relative to their expression in wild-type αLP (vertical black lines indicate genes encoding for the indicated gene sets).

duction, and maintenance (Nurieva et al., 2010). We also identified differential expression of *Zbtb7b* (also known as *Thpok*), *Runx3*, and *Ets1*. Interestingly ETS-1 has been described recently to promote the development of ILC2p in the bone marrow (Zook et al., 2016).

Our study also revealed other surface markers to identify the αLP in adult bone marrow. Importantly, we identified PD-1 as a marker of the $PLZF^+$ ILCp in the bone marrow. This is very interesting because, until now, these cells could only be identified using reporter mice. Our data suggest that the induction of PD-1 on the αLP marks the separation between the ILC and the NK cell lineage because $PLZF^+$ ILCps have lost the NK cell potential, whereas the αLP can generate both lineages (Constantinides et al., 2014; Yu et al., 2014). Interestingly, these markers are important inhibitory receptors of lymphocyte activation. Because PD1 and CD226 function act as a "rheostat" to modulate lymphocyte responses, it is intriguing that these receptors are also expressed on the ILC progenitor. Although we did not find any impairment of ILC development in $Pdcd1^{-/-}$ mice, more investigation will be required to assess the role of these receptors in ILC function.

A key step in defining both the commitment and subsequent specification of ILC depends on NFIL3 and ID2 because these transcription factors have been established as critical regulators of ILC development. Despite this, the exact temporal requirement for these two factors and how they interact have not been fully elucidated. NFIL3 expression is induced by IL-7 originating from mesenchymal cells and is essential for the development of ILC progenitors prior to commitment (Seillet et al., 2014b; Xu et al., 2015). Accordingly, ablation of NFIL3 results in the loss of both $ID2^+$ and $PLZF^+$ ILC progenitors, indicating

permitting us to map the developmental changes of the bone marrow-derived progenitors during differentiation. We identified a specific ILC transcriptional program allowing us to generate a more accurate definition of the different stages of ILC commitment and specification. The transition between the αLP and ILC2p was associated with upregulation of *Il1rl1*, *Il2rα*, *Ly6a*, *CCR9*, and *Klrg1* together with several transcripts that may regulate ILC2 function or development. These included *Socs2*, *Cysltr1*, *Cish*, *Traf4*, and *Rnf128 (*also known as *GRAIL*) (Figure 3C). *Cysltr1* encodes cysteinyl leukotriene receptor 1, which triggers the production of cysteinyl leukotrienes. These factors are critical for the induction of Th2 immunity to allergens in the lung (Barrett et al., 2011), and one could postulate that they represent another important level for regulating ILC2 function. A second gene, *Rnf128*, is an ubiquitin-protein ligase (E3) and an important gatekeeper of T cell responsiveness, tolerance in-

that it exerts its action through the direct binding of NFIL3 at the ID2 locus (Xu et al., 2015). Nevertheless, ID2 expression is not completely lost when NFIL3 is removed (Klose et al., 2014; Robinette et al., 2015; Seillet et al., 2014a). In our studies, N*fil3*-deficient bone marrow exhibited the most profound defect in progenitor development, supporting previous findings. Surprisingly, we found that the loss of NFIL3 function in cells expressing ID2 did not significantly affect the subsequent development of ILC subsets. This result is concordant with the observation that deletion of NFIL3 using Ror$\gamma$t-Cre did not significantly interrupt subsequent ILC development (Xu et al., 2015), and the lack of a requirement for NFIL3 to maintain mature NK cells, ILC1, and ILC3, as reported previously (Firth et al., 2013). Our findings extend these observations and demonstrate that the downstream role of ID2 is also independent of NFIL3. In addition, it reinforces the notion that transient expression of transcriptional regulators such as NFIL3 in ILC progenitors is necessary and sufficient to establish lineage commitment but is subsequently dispensable in controlling ILC development into mature cells.

Collectively, our data establish a genome-wide transcriptional blueprint of the different ILC progenitors and uncover potentially important transcriptional regulators that are likely to reveal key insights into ILC development and interactions with other immune cells in the tissue.

## EXPERIMENTAL PROCEDURES

### Mice

*Tcf7*$^{-/-}$ (Verbeek et al., 1995), *ID2*$^{gfp}$ (Jackson et al., 2011), *Id2*$^{fl/fl}$ (Masson et al., 2013), *VavCre*$^{+/T}$ (Croker et al., 2004), *Nfil3*$^{-/-}$ (Gascoyne et al., 2009), *Nfil3*$^{fl/fl}$ (Motomura et al., 2011), *Rag2*$^{-/-}\gamma_c{}^{-/-}$ (Garcia et al., 1999), B6.129S (Cg)-*Id2*$^{tm1.1\ (cre/ERT2)Blh}$/ZhuJ (Id2-CreERT2) (Rawlins et al., 2009), CD45.1$^{+}$*Eomes*$^{mCherry}$ (Kara et al., 2015), *Pcdc1*$^{-/-}$ (Keir et al., 2007), Irf8$^{egfp}$ (Wang et al., 2014), and PU.1$^{gfp}$ (Nutt et al., 2005) mice have been described previously. C57BL/6, B6.SJL-*Ptprc*$^{a}$ *Pep3*$^{b}$/BoyJ (Ly5.1$^{+/+}$, CD45.1$^{+/+}$) and Ly5.1$^{+}$ × Ly5.2$^{+}$ (F1) mice were bred and maintained in-house. *Id2-CreERT2* mice were crossed to *Nfil3*$^{fl/fl}$ mice to generate *Nfil3*$^{fl/fl}$*Id2-CreERT2*$^{+/T}$ mice (hereafter designated *Nfil3*$^{fl/fl}$*Id2ERT2*$^{+/T}$), and *VavCre*$^{+/T}$ mice were crossed to *Id2*$^{fl/fl}$ mice to generate *Id2*$^{fl/fl}$*VavCre*$^{+/T}$ mice lacking ID2 in the hematopoietic compartment. Estrogen receptor-mediated deletion of loxP-flanked alleles was triggered by the administration of tamoxifen (0.2 mg/g body weight) by oral gavage every 2 days for 10 days. For in vitro experiments, cells were treated with 200 nM 4-hydroxytamoxifen (Sigma-Aldrich). Mice were used at 8–12 weeks of age unless otherwise stated. All animals were maintained and bred under specific pathogen-free conditions and used in accordance with the guidelines of the Walter and Eliza Hall Institute of Medical Research Animal Ethics Committee.

### Isolation and Analyses of Intestinal Lymphocytes

Intestinal lamina propria lymphocytes were isolated from the lamina propria following digestion with Collagenase III (1 mg/mL, Worthington Biochemical), DNase I (200 μg/mL, Roche), and dispase (4 U/mL, Sigma) for 45 min at 37°C. Single-cell suspensions were stained with the following antibodies: TCR$\beta$ (H57-597) from BioLegend; CD19 (ID3), CD3 (145-2C11), ICOS (C398.4A), NKp46 (29A1.4), NK1.1 (PK136), CD117 (2B8), CD127 (A7R34), Sca-1 (D7), and ST2 (RMST2-2) from eBioscience; and CD45.1 (A20) CD45.2 (104), CD90.2 (30-H12), and CD49a (Ha31/8) from BD Biosciences. Intracellular staining was performed using the transcription factor staining buffer set (eBioscience) and antibodies against GATA-3 (TWAJ), Ror$\gamma$t (AFKJS-9), and EOMES (Dan11mag) (eBioscience). LMO4 was identified using rabbit anti-mouse LMO4 (Abcam, Ab133010) followed by fluorescein isothiocyanate (FITC)-conjugated donkey anti-rabbit (Jackson ImmunoResearch). Cells were analyzed using a FACS Fortessa (BD Biosciences), and FlowJo software was used for analysis.

### Isolation and Analysis of Bone Marrow Progenitors

BM cells were isolated from long bones and sternum, filtered through 70-μm cell strainers, and blocked with $\alpha$-CD16/32 (2.4G2) followed by biotinylated anti-IL-7R (CD127) antibody. Cell suspensions were washed and incubated with $\alpha$-biotin magnetic microbeads (Miltenyi Biotec) and enriched for the IL-7R/biotin binding fraction. These cells were then stained for c-kit (2B8), CD127 (A7R34), Sca-1 (D7), Flt3 (A2F10), $\alpha_4\beta_7$ integrin (DATK32), CD25 (PC61.5), and streptavidin. Lineage-positive cells (Lin$^{+}$) were excluded from analyses by staining with antibodies for CD3$\varepsilon$ (145-2C11), B220 (RA3-6B2), CD11b (M1/70), Gr1 (RB6-8C5), TER119, CD49b (DX5), NKp46 (29A1.4), F4/80 (BM8), CD122 (TM-b1), TCR$\beta$ (H57-597), and NK1.1 (PK136). Flow cytometric sorting was performed on a FACS Aria (BD Biosciences).

### Mixed Fetal Liver Chimeras

Ly5.2$^{+}$Ly5.1$^{+}$ wild-type mice were lethally irradiated (2 × 550 rads) and reconstituted with a mixture (ratio of 1:6) of wild-type (Ly5.1$^{+}$) and *Tcf7*$^{-/-}$ (Ly5.2$^{+}$) fetal liver cells. Mice were allowed to reconstitute their hematopoietic system for 8 weeks before use.

### Adoptive Transfer of ILC Progenitors

Different precursor populations were purified from CD45.1$^{+}$, CD45.1$^{+}$*Id2*$^{gfp/gfp}$, or CD45.1$^{+}$EOMES$^{mCherry}$ mice as described above. 0.6-1 × 10$^{3}$ highly purified cells were transplanted into sublethally irradiated (450 rads) *Rag2*$^{-/-}\gamma_c{}^{-/-}$ recipients by lateral tail vein injection. Recipients were analyzed 7–10 weeks after transplant.

### CEL-Seq Primer Design

RT primers were designed with an anchored polyT, a unique bar code, the 5′ Illumina adaptor (as used in the Illumina small RNA kit), and a T7 promoter. The bar codes were eight base pairs (bp) long and designed in groups of four so that the first five nucleotides will have equal representation of all four nucleotides to allow for template generation and crosstalk corrections based on the first four nucleotides read in the Illumina platform. The bar codes were designed so that each pair was different by at least two nucleotides so that a single sequencing error will not produce the wrong bar code.

### Library Generation Using CEL-Seq

100 cells of each population were directly sorted into 384-well plates. Each well contained lysis buffer with a unique primer, ERCC spike-in control, and SuperaseIN RNA inhibitor. CEL-seq libraries were constructed using a protocol described earlier (Hashimshony et al., 2012; Liao et al., 2013). Briefly, double-stranded cDNA libraries were prepared and later pooled together for an in vitro transcription reaction using the Ambion MessageAmp II aRNA amplification kit. Illumina libraries were built following the manufacturer's instructions using the Illumina TruSeq small RNA sample prep kit and sequenced on the Illumina MiSeq and NextSeq platform according to standard protocols for 100-bp single-end sequencing.

### CEL-Seq Data Analysis

For MiSeq and NextSeq sequencing data, the base calling and quality scoring were performed using Illumina's real-time analysis software (versions 1.18.54 and 2.4.6, respectively). FASTQ file generation and de-multiplexing was carried out using MiSeq reporter software (version 2.4.60) and bcl2fastq conversion software (version 2.15.0.4). Reads from the FASTQ files were aligned to the mouse genome (mm10) using Rsubread (version 1.18.0) and summarized at the gene level using the featureCounts procedure (Liao et al., 2014). Subsequent analysis was carried out using the edgeR Bioconductor package. The counts were transformed into counts per million (CPM) to standardize for differences in library size, and filtering was carried out to remove genes that were not expressed in any sample. One outlier sample that did not cluster well with other samples of the same type was removed based on visual inspection of the MDS plots. Data were TMM-normalized, and generalized linear models were fitted using glmFit and the associated pipeline from edgeR (version 3.10.2). Genes were ranked for differential expression using likelihood ratio tests,

and significant genes (FDR < 0.05) were clustered using the K-means algorithm from the stats package in R with $k = 6$ clusters on normalized expression levels to produce clustered expression profiles. Heatmap displays were generated using the $\log_2$ counts per million with batch effects removed using removeBatchEffect from the limma (Ritchie et al., 2015) package and the heatmap.2 function from the gplots (Warnes et al., 2015) package with row scaling.

### Statistical Analysis

A two-tailed Student's t test was performed using Prism (GraphPad) to determine statistical significance.

### Pathway Analysis and GSEA

The GSEA method is available at http://www.broad.mit.edu/ (Subramanian et al., 2007). To test whether gene sets were enriched in pairwise comparisons between CLP and αLP, nominal p values were calculated as well as FDR (q value) based on 1,000 random permutations between gene sets. Results were considered significant when $p < 0.05$ and $q < 0.25$. Signature gene sets were derived from Mingueneau et al. (2013) and Revilla-I-Domingo et al. (2012), and rotation gene set testing was performed using the mroast function in edgeR.

## ACCESSION NUMBERS

The accession number for the RNA-seq data reported in this paper is GEO: GSE75851.

## SUPPLEMENTAL INFORMATION

Supplemental Information includes six figures and three tables and can be found with this article online at http://dx.doi.org/10.1016/j.celrep.2016.09.025.

## AUTHOR CONTRIBUTIONS

C.S., L.A.M., S.H.N., N.D.H., D.B.A.Z., F.F.A., S.C., and G.T.B designed the research, performed the experiments, and analyzed the data. J.G., S.S., M.E.R., and W.S performed bioinformatic analyses of the RNA-seq data. G.T.B. supervised the study. G.T.B and C.S. wrote the manuscript with the help of the other co-authors.

## ACKNOWLEDGMENTS

We thank A. Sharpe (Harvard Medical School) and D. Gray (WEHI) for providing *Pcdc1*$^{-/-}$ mice, H. Morse III (NIH) and H. Wang (NIH) for providing the Irf8$^{egfp}$ mice, and S.L. Nutt for providing PU.1$^{gfp}$ mice for analyses. We thank S.L. Nutt and M. Chopin for helpful discussions and critical review of the manuscript. We are indebted to the facilities of our institute, particularly those responsible for animal husbandry and flow cytometry. N.D.H is a recipient of a melanoma research grant from the Harry J. Lloyd Charitable Trust. G.T.B. is supported by an Australian Research Council Future Fellowship. W.S. is supported by a Centenary Fellowship from the Commonwealth Serum Laboratory, Australia. This work was supported by project grants GNT1027472, 1049407, 1047903, and 1062820 (to G.T.B., N.D.H. and S.H.N.) of the National Health and Medical Research Council (NHMRC) of Australia, The Rebecca L. Cooper Medical Foundation, Victorian State Government Operational Infrastructure Support, and the Australian Government NHMRC IRIIS. S.C. is an employee of Boehringer-Ingelheim.

Received: July 9, 2016
Revised: August 11, 2016
Accepted: September 9, 2016
Published: October 4, 2016

## REFERENCES

Allen, R.D., 3rd, Bender, T.P., and Siu, G. (1999). c-Myb is essential for early T cell development. Genes Dev. *13*, 1073–1078.

Barrett, N.A., Rahman, O.M., Fernandez, J.M., Parsons, M.W., Xing, W., Austen, K.F., and Kanaoka, Y. (2011). Dectin-2 mediates Th2 immunity through the generation of cysteinyl leukotrienes. J. Exp. Med. *208*, 593–604.

Chea, S., Schmutz, S., Berthault, C., Perchet, T., Petit, M., Burlen-Defranoux, O., Goldrath, A.W., Rodewald, H.R., Cumano, A., and Golub, R. (2016). Single-Cell Gene Expression Analyses Reveal Heterogeneous Responsiveness of Fetal Innate Lymphoid Progenitors to Notch Signaling. Cell Rep. *14*, 1500–1516.

Constantinides, M.G., McDonald, B.D., Verhoef, P.A., and Bendelac, A. (2014). A committed precursor to innate lymphoid cells. Nature *508*, 397–401.

Croker, B.A., Metcalf, D., Robb, L., Wei, W., Mifsud, S., DiRago, L., Cluse, L.A., Sutherland, K.D., Hartley, L., Williams, E., et al. (2004). SOCS3 is a critical physiological negative regulator of G-CSF signaling and emergency granulopoiesis. Immunity *20*, 153–165.

Crotta, S., Gkioka, A., Male, V., Duarte, J.H., Davidson, S., Nisoli, I., Brady, H.J., and Wack, A. (2014). The transcription factor E4BP4 is not required for extramedullary pathways of NK cell development. J. Immunol. *192*, 2677–2688.

Delconte, R.B., Shi, W., Sathe, P., Ushiki, T., Seillet, C., Minnich, M., Kolesnik, T.B., Rankin, L.C., Mielke, L.A., et al. (2016). The Helix-Loop-Helix Protein ID2 Governs NK Cell Fate by Tuning Their Sensitivity to Interleukin-15. Immunity *44*, 103–115.

Firth, M.A., Madera, S., Beaulieu, A.M., Gasteiger, G., Castillo, E.F., Schluns, K.S., Kubo, M., Rothman, P.B., Vivier, E., and Sun, J.C. (2013). Nfil3-independent lineage maintenance and antiviral response of natural killer cells. J. Exp. Med. *210*, 2981–2990.

Garcia, S., DiSanto, J., and Stockinger, B. (1999). Following the development of a CD4 T cell response in vivo: from activation to memory formation. Immunity *11*, 163–171.

Gascoyne, D.M., Long, E., Veiga-Fernandes, H., de Boer, J., Williams, O., Seddon, B., Coles, M., Kioussis, D., and Brady, H.J. (2009). The basic leucine zipper transcription factor E4BP4 is essential for natural killer cell development. Nat. Immunol. *10*, 1118–1124.

Guo, X., Qiu, J., Tu, T., Yang, X., Deng, L., Anders, R.A., Zhou, L., and Fu, Y.X. (2014). Induction of innate lymphoid cell-derived interleukin-22 by the transcription factor STAT3 mediates protection against intestinal infection. Immunity *40*, 25–39.

Hashimshony, T., Wagner, F., Sher, N., and Yanai, I. (2012). CEL-Seq: single-cell RNA-Seq by multiplexed linear amplification. Cell Rep. *2*, 666–673.

Hoyler, T., Klose, C.S., Souabni, A., Turqueti-Neves, A., Pfeifer, D., Rawlins, E.L., Voehringer, D., Busslinger, M., and Diefenbach, A. (2012). The transcription factor GATA-3 controls cell fate and maintenance of type 2 innate lymphoid cells. Immunity *37*, 634–648.

Ishizuka, I.E., Chea, S., Gudjonson, H., Constantinides, M.G., Dinner, A.R., Bendelac, A., and Golub, R. (2016). Single-cell analysis defines the divergence between the innate lymphoid cell lineage and lymphoid tissue-inducer cell lineage. Nat. Immunol. *17*, 269–276.

Jackson, J.T., Hu, Y., Liu, R., Masson, F., D'Amico, A., Carotta, S., Xin, A., Camilleri, M.J., Mount, A.M., Kallies, A., et al. (2011). Id2 expression delineates differential checkpoints in the genetic program of CD8α+ and CD103+ dendritic cell lineages. EMBO J. *30*, 2690–2704.

Kara, E.E., McKenzie, D.R., Bastow, C.R., Gregor, C.E., Fenix, K.A., Ogunniyi, A.D., Paton, J.C., Mack, M., Pombal, D.R., Seillet, C., et al. (2015). CCR2 defines in vivo development and homing of IL-23-driven GM-CSF-producing Th17 cells. Nat. Commun. *6*, 8644.

Keir, M.E., Freeman, G.J., and Sharpe, A.H. (2007). PD-1 regulates self-reactive CD8+ T cell responses to antigen in lymph nodes and tissues. J. Immunol. *179*, 5064–5070.

Klose, C.S., Flach, M., Möhle, L., Rogell, L., Hoyler, T., Ebert, K., Fabiunke, C., Pfeifer, D., Sexl, V., Fonseca-Pereira, D., et al. (2014). Differentiation of type 1 ILCs from a common progenitor to all helper-like innate lymphoid cell lineages. Cell *157*, 340–356.

Kondo, M., Weissman, I.L., and Akashi, K. (1997). Identification of clonogenic common lymphoid progenitors in mouse bone marrow. Cell *91*, 661–672.

Lécuyer, E., Larivière, S., Sincennes, M.C., Haman, A., Lahlil, R., Todorova, M., Tremblay, M., Wilkes, B.C., and Hoang, T. (2007). Protein stability and transcription factor complex assembly determined by the SCL-LMO2 interaction. J. Biol. Chem. *282*, 33649–33658.

Liao, Y., Smyth, G.K., and Shi, W. (2013). The Subread aligner: fast, accurate and scalable read mapping by seed-and-vote. Nucleic Acids Res. *41*, e108.

Liao, Y., Smyth, G.K., and Shi, W. (2014). featureCounts: an efficient general purpose program for assigning sequence reads to genomic features. Bioinformatics *30*, 923–930.

Lin, Y.C., Jhunjhunwala, S., Benner, C., Heinz, S., Welinder, E., Mansson, R., Sigvardsson, M., Hagman, J., Espinoza, C.A., Dutkowski, J., et al. (2010). A global network of transcription factors, involving E2A, EBF1 and Foxo1, that orchestrates B cell fate. Nat. Immunol. *11*, 635–643.

Male, V., Nisoli, I., Kostrzewski, T., Allan, D.S., Carlyle, J.R., Lord, G.M., Wack, A., and Brady, H.J. (2014). The transcription factor E4bp4/Nfil3 controls commitment to the NK lineage and directly regulates Eomes and Id2 expression. J. Exp. Med. *211*, 635–642.

Masson, F., Minnich, M., Olshansky, M., Bilic, I., Mount, A.M., Kallies, A., Speed, T.P., Busslinger, M., Nutt, S.L., and Belz, G.T. (2013). Id2-mediated inhibition of E2A represses memory CD8+ T cell differentiation. J. Immunol. *190*, 4585–4594.

Mielke, L.A., Groom, J.R., Rankin, L.C., Seillet, C., Masson, F., Putoczki, T., and Belz, G.T. (2013). TCF-1 controls ILC2 and NKp46+RORγt+ innate lymphocyte differentiation and protection in intestinal inflammation. J. Immunol. *191*, 4383–4391.

Mingueneau, M., Kreslavsky, T., Gray, D., Heng, T., Cruse, R., Ericson, J., Bendall, S., Spitzer, M.H., Nolan, G.P., Kobayashi, K., et al.; Immunological Genome Consortium (2013). The transcriptional landscape of αβ T cell differentiation. Nat. Immunol. *14*, 619–632.

Motomura, Y., Kitamura, H., Hijikata, A., Matsunaga, Y., Matsumoto, K., Inoue, H., Atarashi, K., Hori, S., Watarai, H., Zhu, J., et al. (2011). The transcription factor E4BP4 regulates the production of IL-10 and IL-13 in CD4+ T cells. Nat. Immunol. *12*, 450–459.

Nurieva, R.I., Zheng, S., Jin, W., Chung, Y., Zhang, Y., Martinez, G.J., Reynolds, J.M., Wang, S.L., Lin, X., Sun, S.C., et al. (2010). The E3 ubiquitin ligase GRAIL regulates T cell tolerance and regulatory T cell function by mediating T cell receptor-CD3 degradation. Immunity *32*, 670–680.

Nutt, S.L., Metcalf, D., D'Amico, A., Polli, M., and Wu, L. (2005). Dynamic regulation of PU.1 expression in multipotent hematopoietic progenitors. J. Exp. Med. *201*, 221–231.

Possot, C., Schmutz, S., Chea, S., Boucontet, L., Louise, A., Cumano, A., and Golub, R. (2011). Notch signaling is necessary for adult, but not fetal, development of RORγt(+) innate lymphoid cells. Nat. Immunol. *12*, 949–958.

Rawlins, E.L., Clark, C.P., Xue, Y., and Hogan, B.L. (2009). The Id2+ distal tip lung epithelium contains individual multipotent embryonic progenitor cells. Development *136*, 3741–3745.

Revilla-I-Domingo, R., Bilic, I., Vilagos, B., Tagoh, H., Ebert, A., Tamir, I.M., Smeenk, L., Trupke, J., Sommer, A., Jaritz, M., and Busslinger, M. (2012). The B-cell identity factor Pax5 regulates distinct transcriptional programmes in early and late B lymphopoiesis. EMBO J. *31*, 3130–3146.

Ritchie, M.E., Phipson, B., Wu, D., Hu, Y., Law, C.W., Shi, W., and Smyth, G.K. (2015). limma powers differential expression analyses for RNA-sequencing and microarray studies. Nucleic Acids Res. *43*, e47.

Robinette, M.L., Fuchs, A., Cortez, V.S., Lee, J.S., Wang, Y., Durum, S.K., Gilfillan, S., and Colonna, M.; Immunological Genome Consortium (2015). Transcriptional programs define molecular characteristics of innate lymphoid cell classes and subsets. Nat. Immunol. *16*, 306–317.

Schilham, M.W., Oosterwegel, M.A., Moerer, P., Ya, J., de Boer, P.A., van de Wetering, M., Verbeek, S., Lamers, W.H., Kruisbeek, A.M., Cumano, A., and Clevers, H. (1996). Defects in cardiac outflow tract formation and pro-B-lymphocyte expansion in mice lacking Sox-4. Nature *380*, 711–714.

Seillet, C., Huntington, N.D., Gangatirkar, P., Axelsson, E., Minnich, M., Brady, H.J., Busslinger, M., Smyth, M.J., Belz, G.T., and Carotta, S. (2014a). Differential requirement for Nfil3 during NK cell development. J. Immunol. *192*, 2667–2676.

Seillet, C., Rankin, L.C., Groom, J.R., Mielke, L.A., Tellier, J., Chopin, M., Huntington, N.D., Belz, G.T., and Carotta, S. (2014b). Nfil3 is required for the development of all innate lymphoid cell subsets. J. Exp. Med. *211*, 1733–1740.

Subramanian, A., Kuehn, H., Gould, J., Tamayo, P., and Mesirov, J.P. (2007). GSEA-P: a desktop application for Gene Set Enrichment Analysis. Bioinformatics *23*, 3251–3253.

Verbeek, S., Izon, D., Hofhuis, F., Robanus-Maandag, E., te Riele, H., van de Wetering, M., Oosterwegel, M., Wilson, A., MacDonald, H.R., and Clevers, H. (1995). An HMG-box-containing T-cell factor required for thymocyte differentiation. Nature *374*, 70–74.

Wang, H., Yan, M., Sun, J., Jain, S., Yoshimi, R., Abolfath, S.M., Ozato, K., Coleman, W.G., Jr., Ng, A.P., Metcalf, D., et al. (2014). A reporter mouse reveals lineage-specific and heterogeneous expression of IRF8 during lymphoid and myeloid cell differentiation. J. Immunol. *193*, 1766–1777.

Warnes, G.R., Bolker, B., Bonebakker, L., Liaw, W.H.A., Lumley, T., Maechler, M., Magnusson, A.S.M., Schwartz, M., and Venables, B. (2015). gplots: Various R Programming Tools for Plotting Data. http://CRAN.R-project.org/package=gplots.

Xu, W., and Kee, B.L. (2007). Growth factor independent 1B (Gfi1b) is an E2A target gene that modulates Gata3 in T-cell lymphomas. Blood *109*, 4406–4414.

Xu, W., Domingues, R.G., Fonseca-Pereira, D., Ferreira, M., Ribeiro, H., Lopez-Lastra, S., Motomura, Y., Moreira-Santos, L., Bihl, F., Braud, V., et al. (2015). NFIL3 orchestrates the emergence of common helper innate lymphoid cell precursors. Cell Rep. *10*, 2043–2054.

Yang, Q., Monticelli, L.A., Saenz, S.A., Chi, A.W., Sonnenberg, G.F., Tang, J., De Obaldia, M.E., Bailis, W., Bryson, J.L., Toscano, K., et al. (2013). T cell factor 1 is required for group 2 innate lymphoid cell generation. Immunity *38*, 694–704.

Yang, Q., Li, F., Harly, C., Xing, S., Ye, L., Xia, X., Wang, H., Wang, X., Yu, S., Zhou, X., et al. (2015). TCF-1 upregulation identifies early innate lymphoid progenitors in the bone marrow. Nat. Immunol. *16*, 1044–1050.

Yu, X., Wang, Y., Deng, M., Li, Y., Ruhn, K.A., Zhang, C.C., and Hooper, L.V. (2014). The basic leucine zipper transcription factor NFIL3 directs the development of a common innate lymphoid cell precursor. eLife *3*, 04406.

Zook, E.C., and Kee, B.L. (2016). Development of innate lymphoid cells. Nat. Immunol. *17*, 775–782.

Zook, E.C., Ramirez, K., Guo, X., van der Voort, G., Sigvardsson, M., Svensson, E.C., Fu, Y.-X., and Kee, B.L. (2016). The ETS1 transcription factor is required for the development and cytokine-induced expansion of ILC2. J. Exp. Med. *213*, 687–696.